Novel Automated Manual Transmission Gear-Shift Map Modelling Based on Throttle Position

G. Singh, M. Sharma and A. P. Singh[*]

Mechanical Engineering, UIET, Panjab University, Chandigarh - 160014
*Email: apsingh@pu.ac.in
Phone: +91 9501010029, Fax: +91 172 2547986

ABSTRACT

Automated Manual Transmission (AMT) is capable of providing good driving comfort and performance with increased fuel efficiency of the automobile. In an AMT, gear-shift maps are popularly used for shifting gears. In this work, a novel strategy of shifting gears in an AMT is proposed by utilizing a set of polynomial functions instead of using gear-shift maps directly for shifting the gears. These polynomial functions are precisely extracted from the master gear-shift map of an automobile. Polynomial functions are obtained in MATLAB from gear-shift maps available in literature using curve fitting technique. Mathematical model of a driveline is obtained from free body diagrams of each part. Driveline models are divided into three categories depending on different phases of operation of driveline as: engaged model, slipping model and synchronization model. State-space mathematical models are thereafter derived for each phase. Simulations are done using these state-space models in which polynomial functions are used for gear shifting. Results demonstrate that polynomial functions for gear-shaft maps can be effectively utilized for shifting gears under different loads and throttle positions.

Keywords: Transmission; AMT; gear shift; gear shift map; polynomial; synchronization; Actuator.

INTRODUCTION

Transmission system is a critical sub-system for enhancing efficiency, performance and drivability of an automobile. Two main types of transmissions commonly used in automobiles are Manual Transmission (MT) and Automatic Transmission (AT). MT has higher efficiency, lower cost & weight than AT and gear selection is manually governed by the driver. Frequent gear shifting in congested traffic results in fatigue of the driver. Lesser number of parts makes MT's manufacturing easy, reliable and robust. Mechanical efficiency of MT can be as high as 96 %. In AT, gear-selection is controlled by Transmission Control Unit (TCU). It is easy to operate with good drivability but has higher fuel consumption than MT. Also its manufacturing cost is high, has shorter life time and has high maintenance cost. Mechanical efficiency of AT is very low at about 86 % [1, 2].

Figure 1 shows the schematic diagram of an AMT. In AMT gears are automatically changed based upon speed of vehicle and load on vehicle. AMT consists of a sensor to measure speed of vehicle, actuators to actuate gear levers and a processor to generate control signal as per some control law. Conventionally, AMT with an IC engine has an automated clutch. TCU controls the clutch and gear shifting through

actuators. TCU controls the actuators based upon different vehicle parameters. Use of clutch may result in jerk during shifting process as the speeds of input and output shafts are different. Therefore, many researchers have studied the feasibility of removing clutch and effort is being made to evolve clutchless AMT.
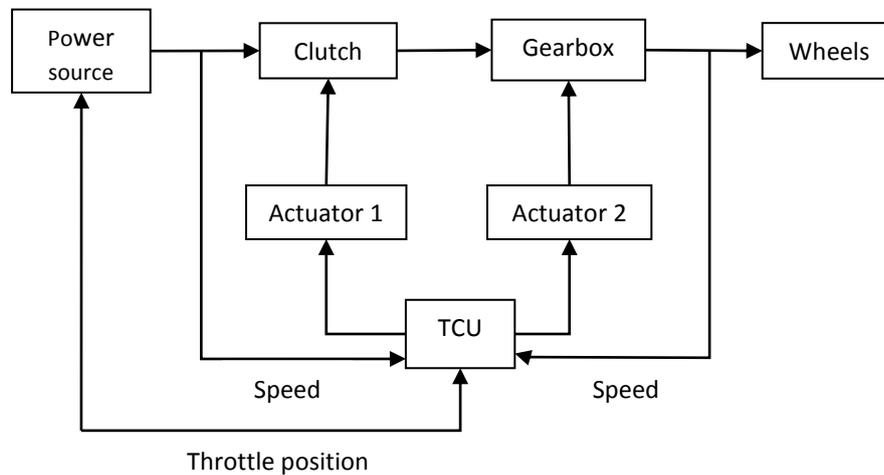
Figure 1. Schematic diagram of a typical AMT.

A typical AMT consists of a power source, a clutch, a gear-box, a controller, actuators and sensors. Torque produced by power source is transmitted to the driveline and a clutch is used to regulate the torque transmitted to driveline. During gear-shifting, force is applied on the clutch disk to regulate the torque transmitted to the driveline. A mathematical model of driveline can be obtained using equations of motions for engine, clutch, transmission and wheels. The derived mathematical model can be easily converted into state space [3,4]. Gearshift quality, drivability, fuel economy can be improved by controlling engine along with actuators for transmission [5]. Shift load on gear lever mainly comes from synchronizer and self-locking mechanism of the fork shaft to avoid voluntary shifting [6]. Shift force transmitted to the driver's hand in a manual transmission can be estimated from stimulation [7]. Detailed non-linear mathematical models for clutch system, gearbox and electro-hydraulic actuators are available [8]. A two degree-of-freedom electromagnetic actuator improves the shift quality and increase the transmission efficiency of gearshift system [9]. Performance analysis of an actuator for clutch operation, based on dc servo motor is available [10]. For a clutchless AMT, a robust position control method can be used for gear actuation to reduce the shifting process time by reducing the time of synchronization phase [1]. A driveshaft torque observer can be used in an AMT [11]. Appreciable amount of torque gap exists when clutch is disengaged for shifting the gears. This torque gap can be considerably removed by using flywheel assisted device that provides uninterrupted connection of load shaft with engine during the gearshift [12]. Gear-shifting can be made smooth using an electro-mechanical friction clutch [13]. A dual-clutch in control-oriented driveline can be used to improve the shift quality and comfort of a vehicle [14]. A starting strategy based on clutch characteristics and throttle control can be used on a vehicle with pneumatic control [15]. To fulfil the clutch engagement requirements, fuzzy control theory can also be used [16]. Use of hybridized automated manual transmission (HAMT) is successfully demonstrated to provide high efficiency, improved drivability and high torque capacity [17].

There are two methods to design a gear shift schedule. First technique uses throttle position and speed of the vehicle to decide gear shifting. Whereas, in second technique; throttle position, speed and acceleration are used to decide the gear shifting. Two parameters-based gear shift schedule is obtained by the intersection of two sets of traction curves i.e. relationship between tractive effort and velocity of vehicle, at different throttle positions. In gear shift schedule based on three parameters, intersection of two sets of acceleration curves (acceleration of vehicle vs. speed of vehicle) at different throttle positions is used [18]. Neuro-fuzzy control approaches are used for optimal gear-shift schedule by estimating the vehicle load and inferring driver's intentions [19]. The MAX-MIN ant algorithm can be used to train back-propagation (BP) neural networks for automating gear shifting in an AMT [20]. Pattern recognition technique can also be applied to simulate gear shifting requirement as done by driver with manual transmission and the shift schedule in AMT can then be optimized using iterative learning algorithm [21]. An optimal fuel economy gear shift schedule can be developed based on three parameters (acceleration, throttle position and speed of vehicle) by studying the fuel consumption of the engine [22]. Engine control unit (ECU) can be used for collecting the sensor signals, recognize the operating pattern of vehicles and control various actions of the actuators [23]. In knowledge-based gear-position-decision (KGPD), an estimator is used to estimate the driving environment & features of driver's intention and is then used for calculating the best gear position [24]. Gear-shifting maps based on different driving modes of parallel hybrid electric vehicle can be generated considering efficiency of induction machine and fuel consumption [25].

In this paper, authors present a novel technique to use gear-shift maps in the form of polynomial expressions in an AMT. The polynomial expressions are obtained from actual gear-shift maps using curve-fitting technique in MATLAB. Main focus of this study is to use these polynomial expressions for shifting gears. Gear-shift maps are highly non-linear, and a single function cannot capture the dynamics of the system. Therefore, this work presents a novel strategy to effectively capture the dynamics by dividing the throttle opening from fully closed to fully open into three segments and separate functions are derived to effectively capture the behaviour. A full driveline model is used in MATLAB to simulate the gear-shifting using polynomial expressions for different throttle positions, input torque values and load torque values.

DRIVELINE MODELLING

In a vehicle, power from engine is transmitted through flywheel, clutch, main shaft, gearbox, propeller shaft, differential and then through drive shaft to the wheels. Engine, clutch, flywheel, main shaft, gearbox, differential, driveshaft and wheels collectively make the driveline of a vehicle.

For understanding dynamics of a driveline, a simplified driveline is considered as shown in Figure 2. Every component is studied separately i.e., crankshaft, clutch, main shaft and wheels. In Figure 2, J_e, J_c, J_m, J_s, J_g, J_p, J_f and J_w are rotational inertia of engine, clutch, main shaft, secondary shaft, gear engaged, pinion, final drive (differential) and wheels respectively. Secondary shaft inertia is sum of inertia of all gears (J_{s1}, J_{s2}, J_{s3}, and J_{s4}) on it. θ represents rotation where subscripts 'e' represents engine, 'c' is for clutch, 'm' is for main shaft, 't' is for transmission, 'f' is for final drive and 'w' is for wheels. Gear ratio i_s is for secondary shaft, i_g for transmission shaft and i_f for final drive. Following assumptions are used to obtain the driveline model:

a) All the shafts are assumed as mass-less and the whole system is made up of lumped masses acting on the ends of the shafts.
b) There is no friction acting on the crankshaft.
c) Driveshaft and clutch are assumed to be flexible.
d) Load on wheels due to the air resistance and rolling resistance is assumed to be negligible.
e) Rotational inertias in the transmission line are assumed to be constant.
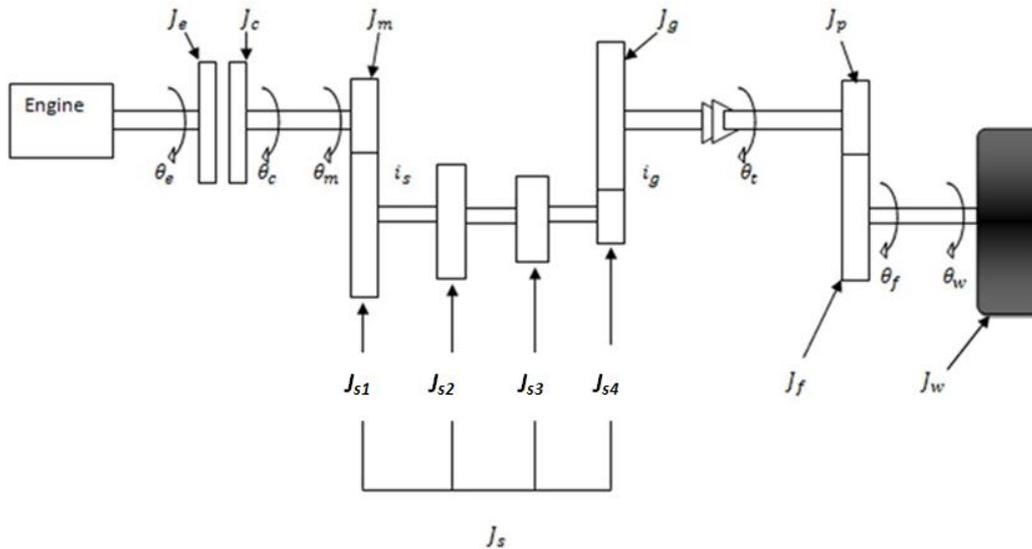
Figure 2. Simplified schematic of automotive driveline.

Free-body Diagram (FBD)

FBDs showing different forces are drawn for different parts of vehicle driveline. Each part is considered under effect of inertia torque, driving torque, resistive torque and load torque. Equations of motion are derived for each part from equilibrium conditions.

Crank shaft

Crankshaft is considered as rigid shaft under the effect of driving torque from engine, load torque from clutch and assuming that no friction torque is acting on it. Inertia of the engine and flywheel is the total inertia acting on the shaft. Motion of crank shaft can be derived from free body diagram shown in Figure 3 (a) as in Eq. (1).

$$J_e\ddot{\theta}_e = T_e - T_c \tag{1}$$

where T_e is engine torque and T_c is load torque on shaft due to friction between clutch disks.

Clutch

Main shaft and driveshaft are the main flexibilities in a driveline. Main shaft is modelled as damped torsional flexibility resisting rotation of clutch. Motion of clutch can be derived from free body diagram shown in Figure 3 (b) as Eq. (2).

$$J_c\ddot{\theta}_c = T_c - k_{cm}(\theta_c - \theta_m) - \beta_{cm}(\dot{\theta}_c - \dot{\theta}_m) \tag{2}$$

where k_{cm} is main shaft torsional stiffness and β_{cm} is friction coefficient of main shaft.

Main shaft

Load torque acting on the main shaft (shown in Figure 4) is load torque acting on the final drive divided by gear ratio.

(a)

(b)
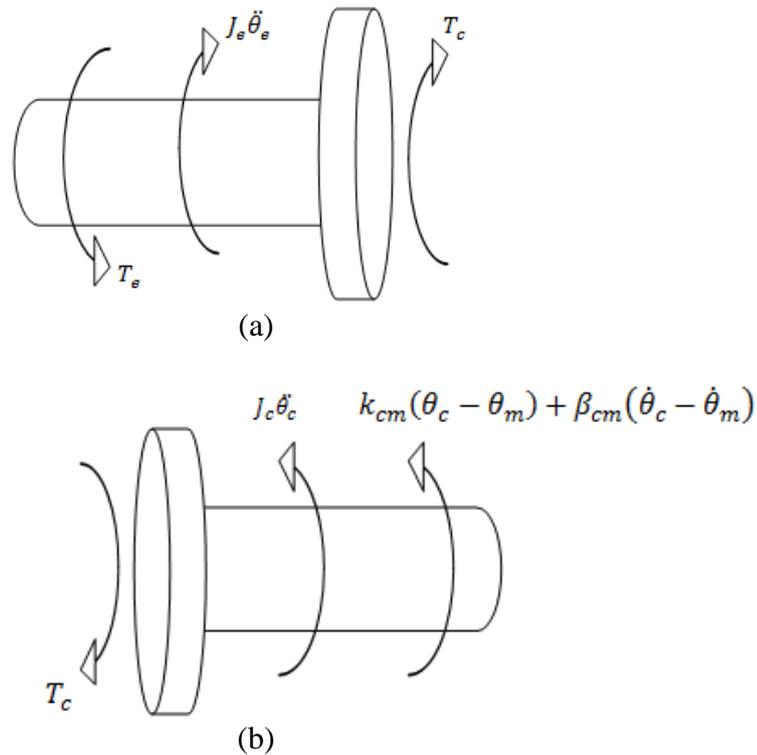
Figure 3. Free-body diagram of the (a) crankshaft and; (b) clutch.
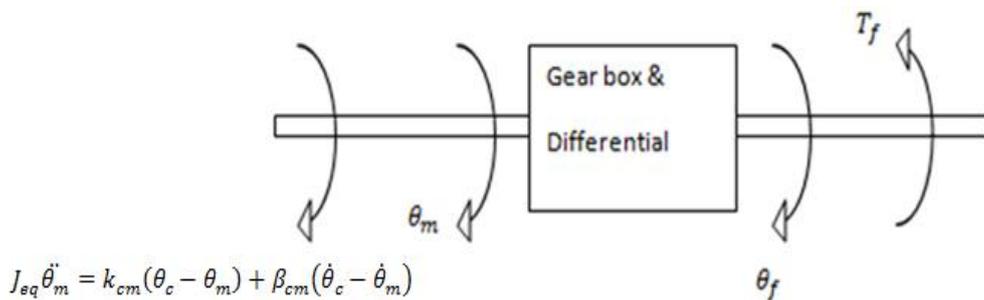
Figure 4. Torques acting on gear box, differential and main shaft.

Here, $T_f = k_{tw}\left(\dfrac{\theta_m}{i_s i_g i_d} - \theta_w\right) + \beta_{tw}\left(\dfrac{\theta_m}{i_s i_g i_d} - \dot{\theta}_w\right)$ is load torque at final drive due to stiffness and damping of driveshaft and $\dfrac{\theta_m}{i_s i_g i_d} = \theta_f$, k_{tw} is torsional stiffness of driveshaft and β_{cm} is friction coefficient of driveshaft.

Equivalent inertia

To obtain main shaft dynamics, inertia of gear box and final drive are summed up in a single quantity known as equivalent inertia. From Figure 2, we can write the following by summing up kinetic energies of individual inertias:

$$\frac{1}{2}(J_{eq}\omega_m^2)=\frac{1}{2}(J_m\omega_m^2)+\frac{1}{2}(J_s\omega_s^2)+\frac{1}{2}(J_g\omega_t^2)+\frac{1}{2}(J_p\omega_t^2)+\frac{1}{2}(J_f\omega_f^2)$$

Equivalent inertia can be represented as Eq. (3) and (4).

$$J_{eq}=J_m+J_s\left(\frac{\omega_s^2}{\omega_m^2}\right)+J_g\left(\frac{\omega_t^2}{\omega_m^2}\right)+J_p\left(\frac{\omega_t^2}{\omega_m^2}\right)+J_f\left(\frac{\omega_f^2}{\omega_m^2}\right) \tag{3}$$

$$J_{eq}=J_m+\frac{J_s}{i_s^2}+\frac{J_g}{i_s^2i_g^2}+\frac{J_p}{i_s^2i_g^2}+\frac{J_f}{i_s^2i_g^2i_f^2} \tag{4}$$

From the free-body diagram shown in Figure 6 (a), torque equation of motion of main shaft is obtained as Eq. (5).

$$J_{eq}\ddot{\theta}_m=k_{cm}(\theta_c-\theta_m)+\beta_{cm}(\dot{\theta}_c-\dot{\theta}_m)-\frac{1}{i_si_gi_d}\left\{k_{tw}\left(\frac{\theta_m}{i_si_gi_d}-\theta_w\right)+\beta_{tw}\left(\frac{\dot{\theta}_m}{i_si_gi_d}-\dot{\theta}_w\right)\right. \tag{5}$$

(a)

(b)
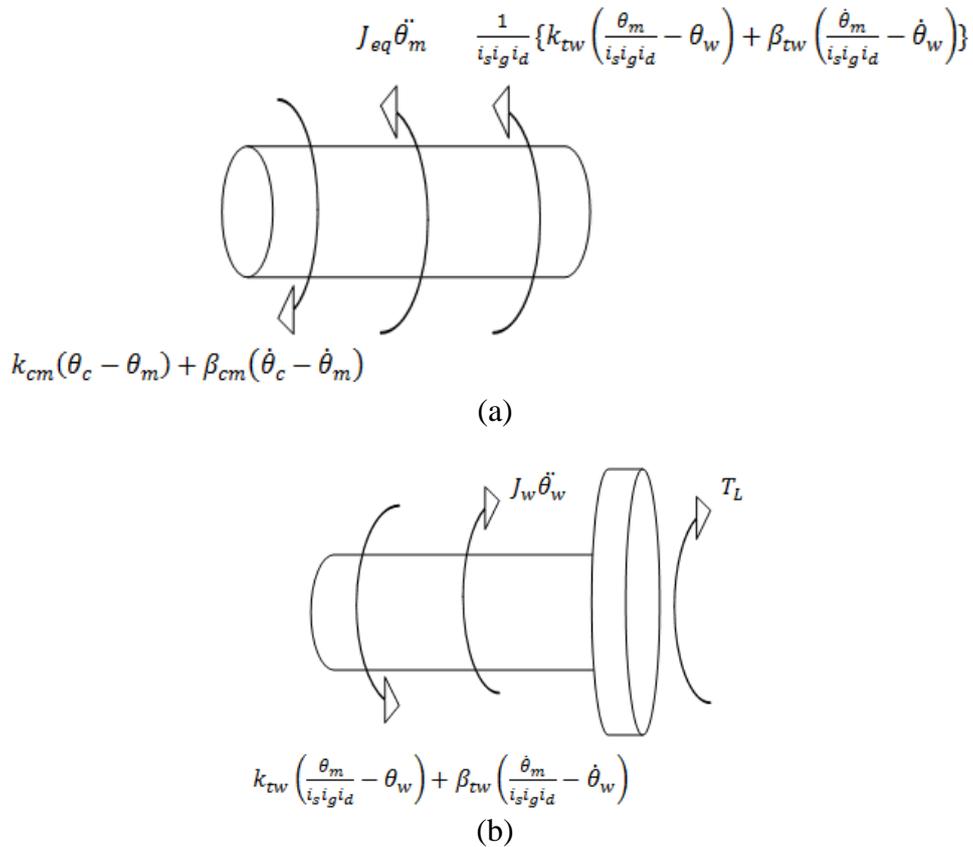
Figure 6. Free-body diagram of the (a) main shaft and; (b) wheel.

Wheels

Total load acting on wheels is due to air resistance, rolling resistance and gravitational forces. In this research work total load due to all these forces is assumed to be constant. From free body diagram shown in Figure 6 (b), equation of motion of wheel is derived as Eq. (6).

$$J_w\ddot{\theta}_w = k_{tw}\left(\frac{\theta_m}{i_s i_g i_d} - \theta_w\right) + \beta_{tw}\left(\frac{\dot{\theta}_m}{i_s i_g i_d} - \dot{\theta}_w\right) - T_L \qquad (6)$$

Where T_L is the load torque on wheels.

AMT Operating Phases

A driveline operates in different phases according to different clutch and gear lever positions. These phases are (1) gear engagement, (2) start of slip (3) synchronization (4) slip phase (5) end of slip as shown in Figure 7. In gear engagement phase, clutch is in engaged position and rotates with same angular velocity as of crankshaft with zero slip. Adding Eq. (1) and (2) we get Eq. (7).

$$(J_e + J_c)\ddot{\theta}_e = T_e - k_{cm}(\theta_c - \theta_m) - \beta_{cm}(\dot{\theta}_c - \dot{\theta}_m) \qquad (7)$$

Equation (7) with Eq. (5) and (6) give driveline dynamics during engaged phase. During start of slip and slip phase, the clutch is not fully engaged. It is either opening or closing and crankshaft speed and clutch speed are not same. Equation (1), (2), (5) and (6) represent driveline in these two phases. Slipping phase is followed by end of slip, in which clutch torque is restored to its maximum value by spring action on pressure plate of clutch.
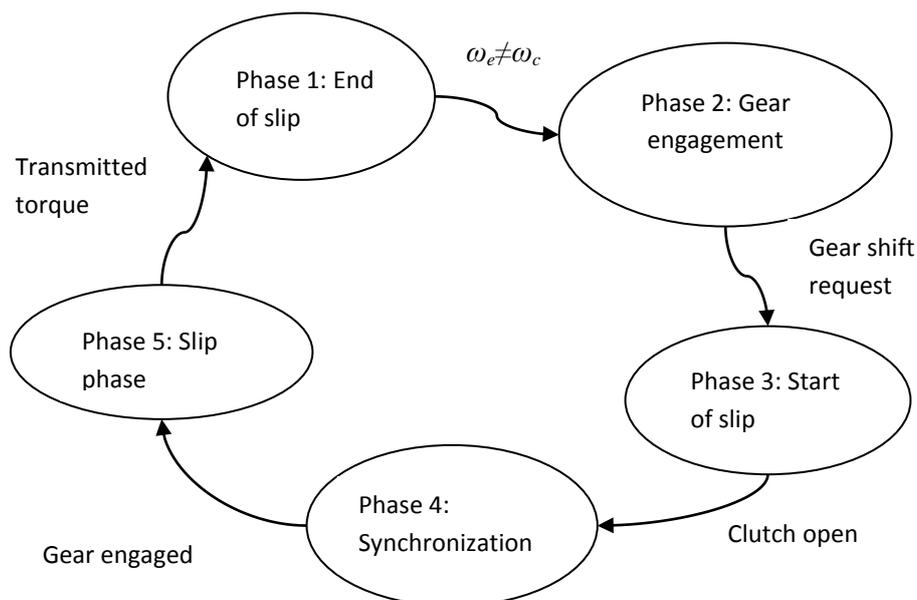
Figure 7. Transition state diagram [26].

In synchronization phase, a new gear to be engaged is acted upon by synchronization torque through gear lever. During this, clutch is fully disengaged and there is no resisting torque on crankshaft and driving torque on main shaft. During synchronization, vehicle speed is assumed to remain constant. Driveline dynamics during this phase is expressed as Eq. (8), (9) and (10).

$$J_e\ddot{\theta}_e = T_e \tag{8}$$

$$J_c\ddot{\theta}_c = -k_{cm}(\theta_c - \theta_m) - \beta_{cm}(\dot{\theta}_c - \dot{\theta}_m) \tag{9}$$

$$J'_{eq}\ddot{\theta}_m = k_{cm}(\theta_c - \theta_m) + \beta_{cm}(\dot{\theta}_c - \dot{\theta}_m) - T_s \tag{10}$$

Where T_s is synchronization torque and J'_{eq} is equivalent inertia without inertia of final drive (i.e. $J\_eq^{'} = J\_m + J\_s/(i\_{(s)}^2) + J\_g/(i\_s^2\,i\_g^2)$).

State-space Models

The input to the system is $u = T_e$, (i.e. engine output torque). Angular velocity of all inertia and angular differences of flexible shafts are state variables of the system.

Engaged model

As explained earlier, in engaged phase speed of engine ($\dot{\theta}_e$) is equal to clutch speed ($\dot{\theta}_c$). From Eq. (5), (6) and Eq.(7) clutch-engaged state space model can be represented mathematically as Eq. (11):

$$\dot{x} = AE.x + BE.u + CE.l \tag{11}$$

Where *AE* is system matrix, *BE* is control matrix, *CE* is load matrix and various state-variables are:
$$x(1,1) = \theta_c - \theta_m$$
$$x(2,1) = \frac{\theta_m}{i_s i_g i_d} - \theta_w$$
$$x(3,1) = \dot{\theta}_e = \dot{\theta}_c$$
$$x(4,1) = \dot{\theta}_m$$
$$x(5,1) = \dot{\theta}_w$$

where,

$$AE = \begin{pmatrix} 0 & 0 & 1 & -1 & 0 \\ 0 & 0 & 0 & 1/i & -1 \\ -\dfrac{K_{cm}}{J_1} & 0 & \dfrac{-\beta_{cm}}{J_1} & \dfrac{\beta_{cm}}{J_1} & 0 \\ \dfrac{K_{cm}}{J_2} & -\dfrac{K_{tw}}{J_2 i} & \dfrac{\beta_{cm}}{J_2} & -\dfrac{\beta_{cm}}{J_2} - \dfrac{\beta_{tw}}{J_2} & \dfrac{\beta_{tw}}{J_2} \\ 0 & \dfrac{K_{tw}}{J_3} & 0 & \dfrac{\beta_{tw}}{J_3} & \dfrac{-\beta_{tw}}{J_3} \end{pmatrix}, \tag{12}$$

$$BE=\begin{pmatrix} 0 \\ 0 \\ 1/J_1 \\ 0 \\ 0 \end{pmatrix} \text{ and } CE=\begin{pmatrix} 0 \\ 0 \\ 0 \\ 0 \\ -1/J_4 \end{pmatrix}$$

where $i=i_s i_g i_d$, $J_1=J_e+J_c$, $J_2=J_{eq}$, $J_3=J_w$, $u = T_e$ and $l = T_L$ is the load acting on wheels.

Slipping model

During slipping, clutch speed and crankshaft speed are not same, i.e. $\omega_e \neq \omega_c$. Moreover, a torque T_c also acts on both sides of the clutch as loading torque and driving torque on crankshaft and clutch respectively. This is less than its maximum value, i.e. $T_c < T_{max}$. State-space representation becomes

$$\dot{x}=ASL.x+BSL.u+CSL.l+DSL.H \tag{13}$$

where $H=T_c$ is the clutch torque, *ASL* is system matrix, *BSL* is control matrix, *CSL* is load matrix and state-variables are

$$x(1,1) = \theta_c - \theta_m$$
$$x(2,1) = \frac{\theta_m}{i_s i_g i_d} - \theta_w$$
$$x(3,1) = \dot{\theta}_e$$
$$x(4,1) = \dot{\theta}_c$$
$$x(5,1) = \dot{\theta}_m$$
$$x(6,1) = \dot{\theta}_w$$

$$ASL=\begin{pmatrix} 0 & 0 & 0 & 1 & -i & 0 \\ 0 & 0 & 0 & 0 & 1 & -1 \\ 0 & 0 & 0 & 0 & 0 & 0 \\ -\frac{K_{cm}}{J_2} & 0 & 0 & \frac{-\beta_{cm}}{J_2} & \frac{\beta_{cm}}{J_2} & 0 \\ \frac{K_{cm}}{J_3} & \frac{-K_{tw}}{J_3 i} & 0 & \frac{\beta_{cm}}{J_3} & -\frac{\beta_{cm}}{J_3}-\frac{\beta_{tw}}{J_3.i^2} & \frac{\beta_{tw}}{J_3.i} \\ 0 & \frac{K_{tw}}{J_4} & 0 & 0 & \frac{\beta_{tw}}{J_4.i} & \frac{-\beta_{tw}}{J_4} \end{pmatrix}^{'},$$

$$BSL=\begin{pmatrix} 0 \\ 0 \\ 1/J_1 \\ 0 \\ 0 \\ 0 \end{pmatrix}, CEL=\begin{pmatrix} 0 \\ 0 \\ 0 \\ 0 \\ 0 \\ -1/J_4 \end{pmatrix} \text{ and } DSL=\begin{pmatrix} 0 \\ 0 \\ -1/J_1 \\ 1/J_1 \\ 0 \\ 0 \end{pmatrix} \tag{14}$$

where $J_1=J_e$, $J_2=J_c$, $J_3=J_{eq}$ and $J_4=J_w$.

Synchronization model

During synchronization, friction between gear cone and synchronizer ring plays a very crucial role as synchronization torque (T_s). For this phase, state-space representation from Eq. (8), (9) and (10) is in Eq. (15).

$$\dot{x}=AS.x+BS.u+ES.P \qquad (15)$$

where $P=T_s$, AS is system matrix, BS is control matrix and ES is load matrix. State-variables are:

$x(1,1)=\theta_c-\theta_m$

$x(2,1)=\dot{\theta}_e$

$x(3,1)=\dot{\theta}_c$

$x(4,1)=\dot{\theta}_m$

$$AS=\begin{pmatrix} 0 & 0 & 1 & -1 \\ 0 & 0 & 0 & 0 \\ -\dfrac{K_{cm}}{J_2} & 0 & \dfrac{-\beta_{cm}}{J_2} & \dfrac{\beta_{cm}}{J_2} \\ \dfrac{K_{cm}}{J_3} & 0 & \dfrac{\beta_{cm}}{J_3} & \dfrac{-\beta_{cm}}{J_3} \end{pmatrix}, BS=\begin{pmatrix} 1/J_1 \\ 0 \\ 0 \\ 0 \end{pmatrix} \text{ and } ES=\begin{pmatrix} 0 \\ 0 \\ 0 \\ -1/J_3 \end{pmatrix} \qquad (16)$$

where $J_1=J_e$, $J_2=J_c$ and $J_3=J'_{eq}$. The values of model parameters used are as follows: $k_{cm}=3200$ Nm/rad, $b_{cm}=4$ Nms/rad, $k_{tw}=16000$ Nm, $b_{tw}=9\ 0$ Nms/rad, $J_e=0.1749$ kgm^2, $J_c=0.0159$ kgm^2, $J_{eq}=0.06$ kgm^2 and $J_w=14$ kgm^2 and gear ratios (i) = 13.65, 7.7, 4.9, 3.5 and 2.45.

GEAR SHIFT STRATEGY

Conventional gear shift schedule (Figure 9) is designed to make available the maximum traction at the wheels of the vehicle. The gear shifting is scheduled to take place at speed corresponding to the intersection of two contiguous traction curves of two different gears at the same throttle position. If there is no intersection of the curves, then the maximum speed of the lower gear will be the speed of the gear shift. In Figure 9 gear shift curves are shown through the intersection of two contiguous gears. For a particular gear, three curves for 90 % throttle position, 60 % throttle position and 30 % throttle position are shown in Figure 9.

Gear-shift using gear map is based upon up-shift curves and downshift curves. In Figure 10, up-shift and downshift for different throttle positions are shown with solid curves and dashed curves respectively. Gear up-shifts or downshifts for a particular throttle position when vehicle reaches up-shift or down-shift speed based upon up-shift or down-shift curves respectively [14].
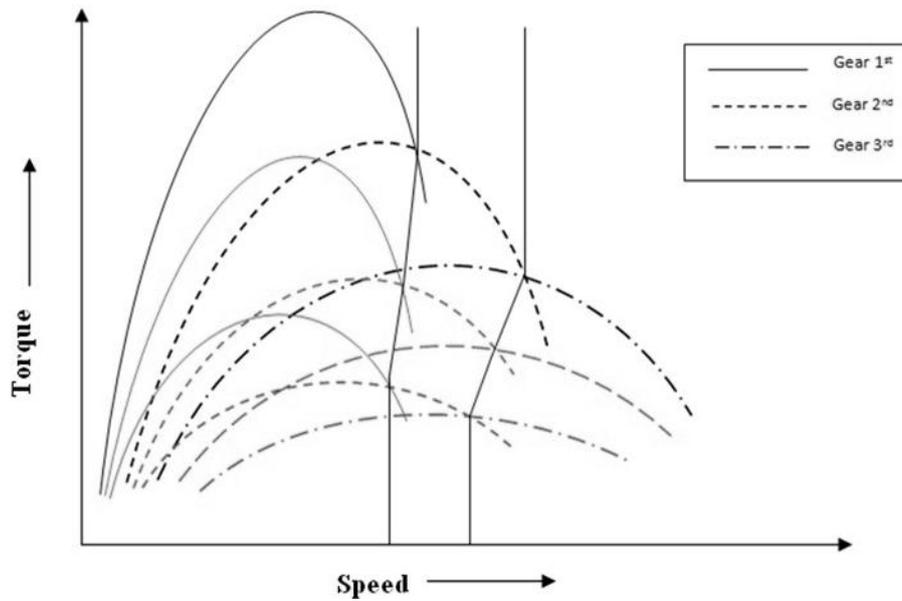
Figure 9. Gear shift curves for automobile transmission.
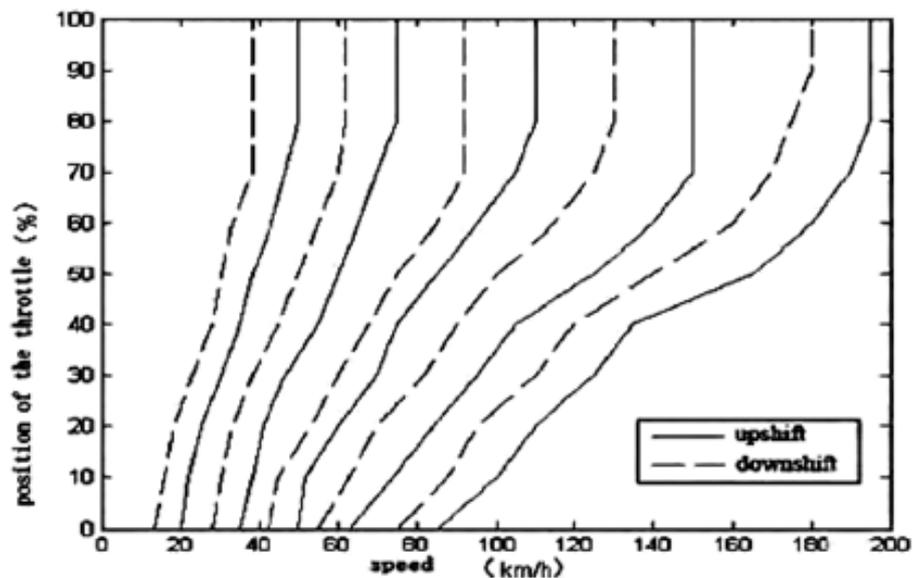
Figure 10. Conventional gear-shift schedules [18].

GEAR-SHIFT POLYNOMIAL FUNCTIONS

Gear maps used for gear shifting are highly non-linear. In this research work, each non-linear graph is divided into three parts and a polynomial function is obtained for each part. This polynomial function takes in throttle position as input and gives gear up shift speed as output depending upon engaged gear. Actual gear shift maps are available from literature. From these maps a set of data values are obtained for each curve. These values are utilized in MATLAB with "polyfit" and "polyval" commands to obtain three polynomial functions for individual gear shift curve. In this way, a full gear shift curve

is obtained from these polynomial functions. Gear up shift map between throttle opening and vehicle speed is shown in Figure 11.

Curves obtained above can be approximated using polynomial functions for different throttle positions as shown in Table 1.

Table 1. Polynomial functions for gear shift map curves

Curves	Fractional opening of throttle	Polynomial
curve for gear 1 to 2	0.1-0.55	$f1=(0.7073y^5-1.1493y^4+0.6925y^3-0.1909y^2+0.023x+.001)*1.0e+05$
	0.55-0.8	$g1=(-0.3219y^5+1.0692y^4-1.4124y^3+0.9277y^2-0.3031y+0.0394)*1.0e+07$
	0.8-1	$h1=86.2y-258.62$
curve for gear 2 to 3	0.1-0.55	$f2=(1.6968y^5-1.6962y^4+0.322y^3+0.1215y^2-0.0374y+0.0396)*1.0e+04$
	0.55-0.8	$g2=(0.3867y^5-2.8987y^4+6.325y^3-6.0139y^2+2.641y-0.436)*1.0e+05$
	0.8-1	$h2=362.09y+293.078$
curve for gear 3 to 4	0.1-0.55	$f3=(2.0943y^5-3.3261y^4+2.0092y^3-0.5726y^2+0.0781y+.002)*1.0e+06$
	0.55-0.8	$g3=(-1.3803y^5+4.4859y^4-5.7686y^3+3.6674y^2-1.1520y+0.1436)*1.0e+06$
	0.8-1	$h3=(1.8966y-0.6897)*1.0e+03$
curve for gear 4 to 5	0.1-0.55	$f4=(1.7438y^5-2.3209y^4+1.1303y^3-0.2494y^2+0.0270y+0.0084$
	0.55-0.8	$g4=(0.3476y^5-1.1266y^4-1.4482y^3+0.9227y^2-0.2912y+0.0365)*1.0e+07$
	0.8-1	$h4=(3.1034y-1.0690)*1.0e+03$

Here, 'y' represents throttle opening. Gear shift map obtained using above polynomial equations are as shown in Figure 11. It is clear from Figure 11 that polynomial functions tabulated in Table 1 are able to accurately model the gear-shift maps.
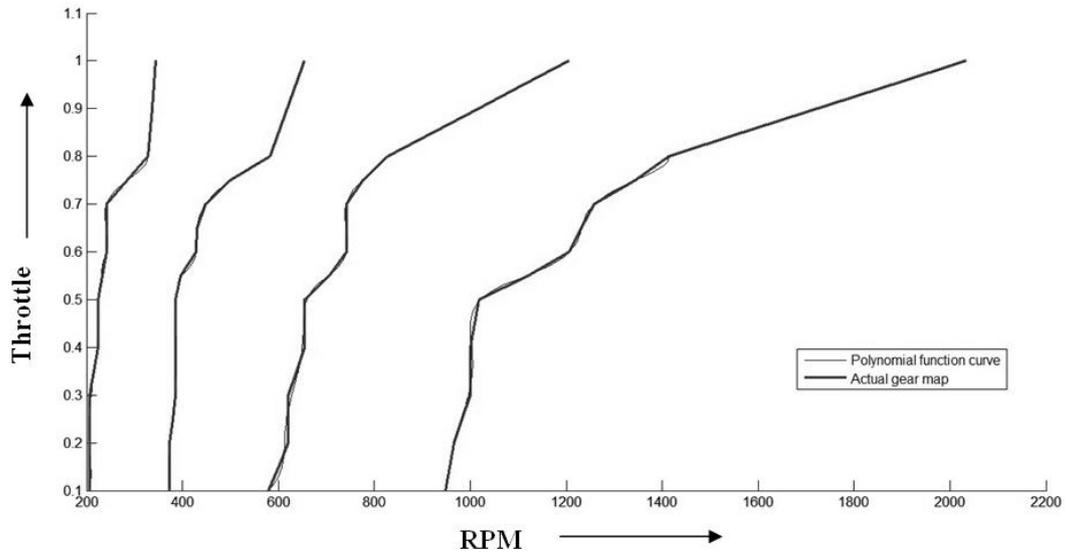
Figure 11. Gear shift map obtained from polynomials functions.

RESULTS AND DISCUSSION

State-space models of driveline are used to simulate the driveline and gear shifting in MATLAB. When in a particular gear, driveline is considered to be in engaged phase and accordingly engaged state-space is used in MATLAB code. During gear shifting process, on gear shift command, engaged model is followed up by slipping model, slipping model by synchronization model, synchronization model again by slipping model and finally slipping model by engaged model in MATLAB code.
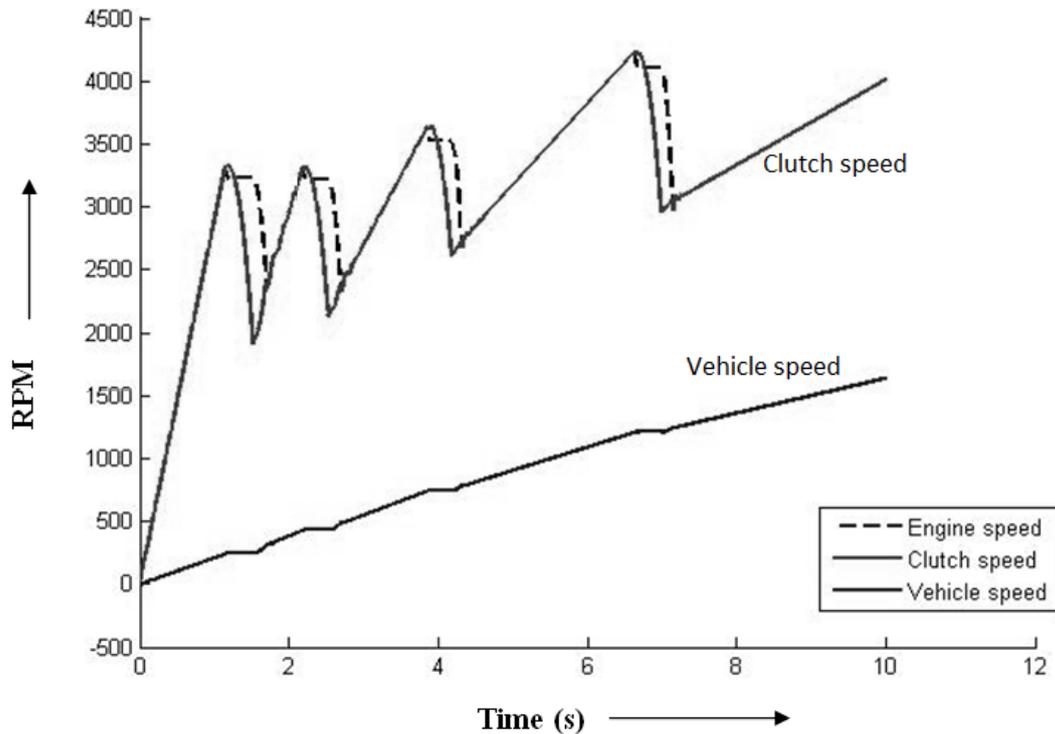
Figure 12. Time response of engine, clutch and vehicle speeds at 60 % throttle opening.

A gear shifting strategy based upon polynomial functions of gear up shift curves is developed in MATLAB. This gear shift strategy takes throttle position, vehicle RPM and engaged gear as input and based upon these inputs, it gives command signal for gear shifting. This gear shift strategy is implemented with driveline for shifting gears.

Engine torque of 100 Nm is applied as input with constant load torque of 20 Nm on wheels. Results of the MATLAB code for simulation time of 10 seconds are shown in Figure 12. Initially gear is in 1ˢᵗ gear. Vehicle speed keeps on increasing with torque applied while gear upshifts from 1ˢᵗ gear to 5ᵗʰ gear. Engine speed and clutch speed remains same during engagement phase. During gearshift, clutch speed and engine speed varies differently according to slipping phase and synchronization phase. Vehicle speed remains constant during synchronization phase.
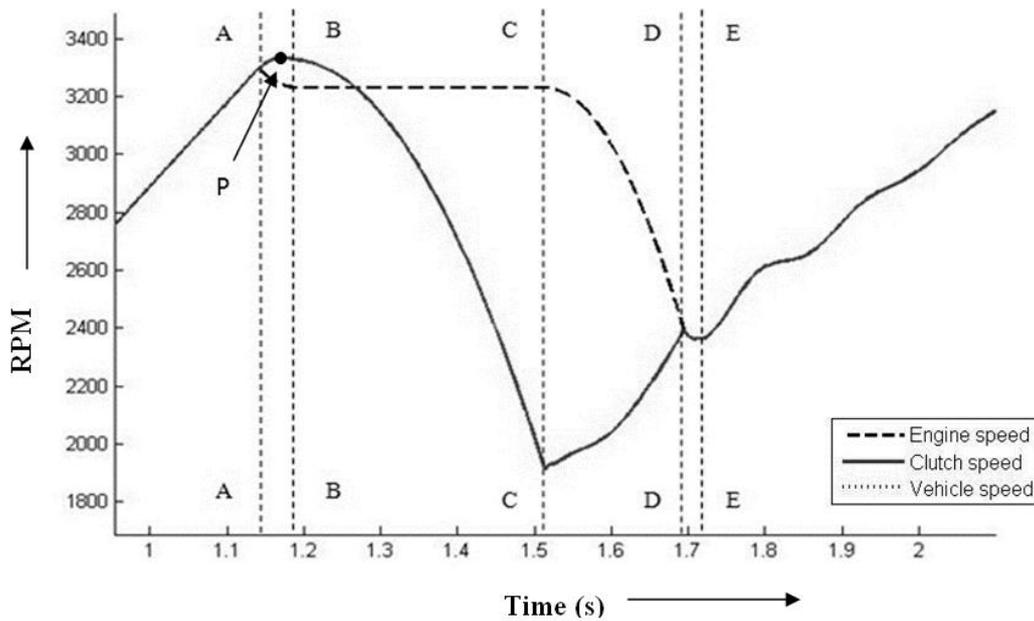
Figure 13. Zoomed view of up-shift from 1ˢᵗ to 2ⁿᵈ gear.

Gear-shifting from 1ˢᵗ to 2ⁿᵈ gear-ratio is shown in Figure 13. On gear-shifting requirement at A-A, engine torque immediately drops to zero and clutch starts to disengage. As there is no engine torque available on the crankshaft and also load torque is coming down due to clutch being disengaged, the speed of crankshaft decreases. As the clutch is disengaging, the frictional torque available on the mainshaft due to clutch is decreasing, which increases mainshaft speed up to point P. At B-B, clutch is fully open, and torque transmitted by it is zero. After this, synchronization phase starts, and synchronization torque applied at synchronizer decreases the clutch speed while engine speed remains constant as there is no input torque and load torque on crankshaft. At C-C gear is synchronized and after it, clutch starts to engage till both engine and clutch speed become same. From C-C to D-D, clutch speed rises while engine speed decreases further due to clutch engagement. After fully engaged clutch at D-D, clutch lock up phase starts, and no engine torque is applied during this phase but only load torque on wheels. Due to this, both engine and clutch speed decreases till E-E. At E-E, gear shifting ends and 2ⁿᵈ gear-ratio is engaged, and torque of engine is again set to 100 Nm.

In Figure 14, gear-shifting from 1ˢᵗ to 5ᵗʰ gear-ratio is shown at 60 % throttle opening and 100 Nm constant engine torque with three different constant load torques

of 150 Nm, 100 Nm and 20 Nm acting on wheels. Variation in gear shift timing of a particular gear is due to the difference in load torques on wheels. More time is required, at same throttle and speed, for shifting a particular gear with higher load torques of 150 Nm and 100 Nm than lower load torque of 20 Nm at wheels.

A similar curve is also obtained when three different constant engine torques of 100 Nm, 150 Nm and 200 Nm are applied as shown in Figure 15. With higher engine torque of 200 Nm, gear shift time from 1st to 5th gear is greatly reduced than that is required for engine torque of 100 Nm at same operating conditions of throttle opening.

Three different gear shift curves for different throttle positions of 90, 60 and 35 % throttle opening are shown in Figure 16. Throttle positions are so chosen that each one of them stimulates all three polynomial functions for a particular gear shift map curves. At higher throttle positions, gear shifting occurs at higher engine/vehicle speed for each gear based on gear shift polynomials.

Gear-shift is also stimulated for sudden load torque and varying load torque acting on the vehicle. In both, sudden increase in load torque and varying load torque, there is appreciable increment in time required for shifting from 1st to 5th gear. In Figure 17, sudden increment in vehicle load torque is shown. Load torque is suddenly increased from 20 Nm to 80 Nm at 2nd second. In Figure 18, gear-shift for sudden increment in load torque is shown. Dashed line curve is for sudden load torque condition and curve with solid line is for constant load torque of 20 Nm.
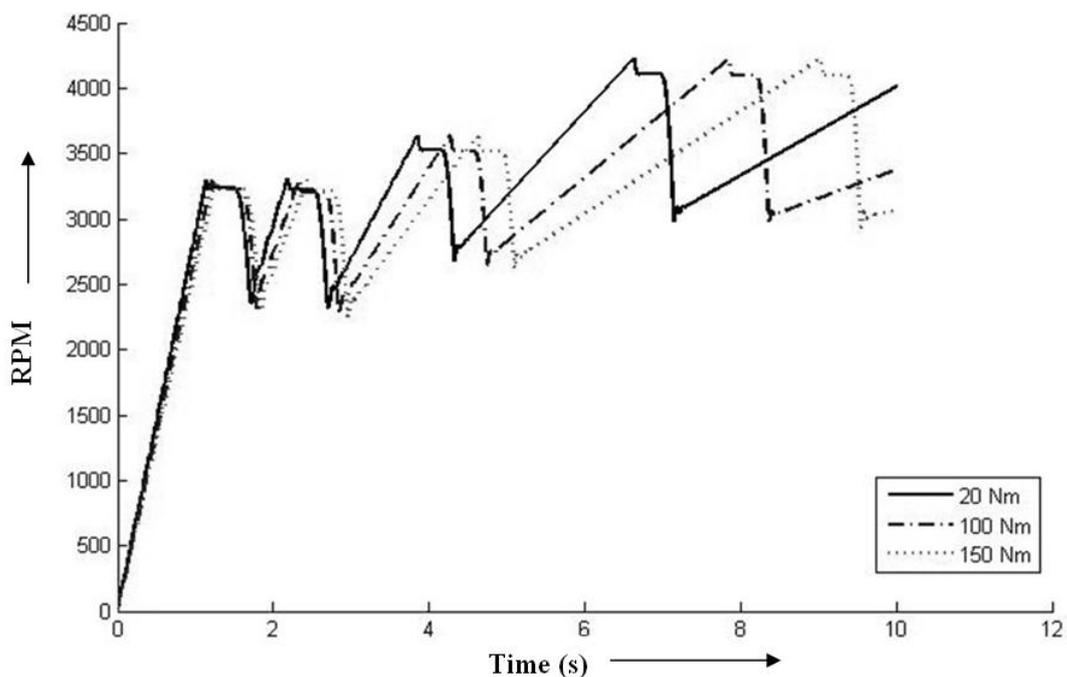
Figure 14. Time response of engine speed at three different load torques.
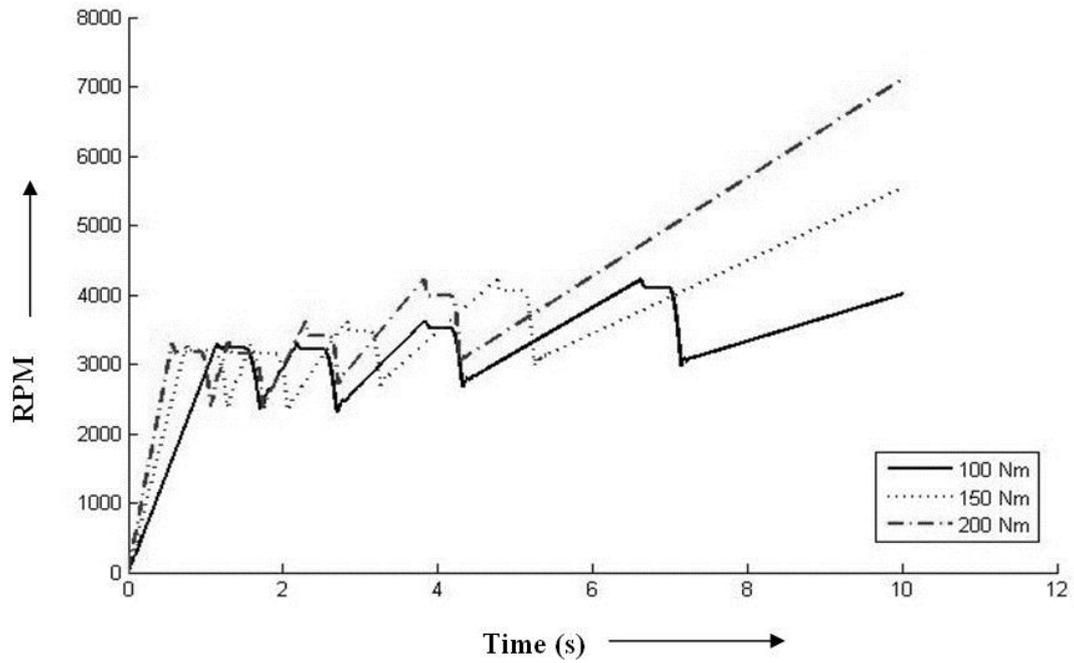
Figure 15. Time response of engine speed at three different input torques.
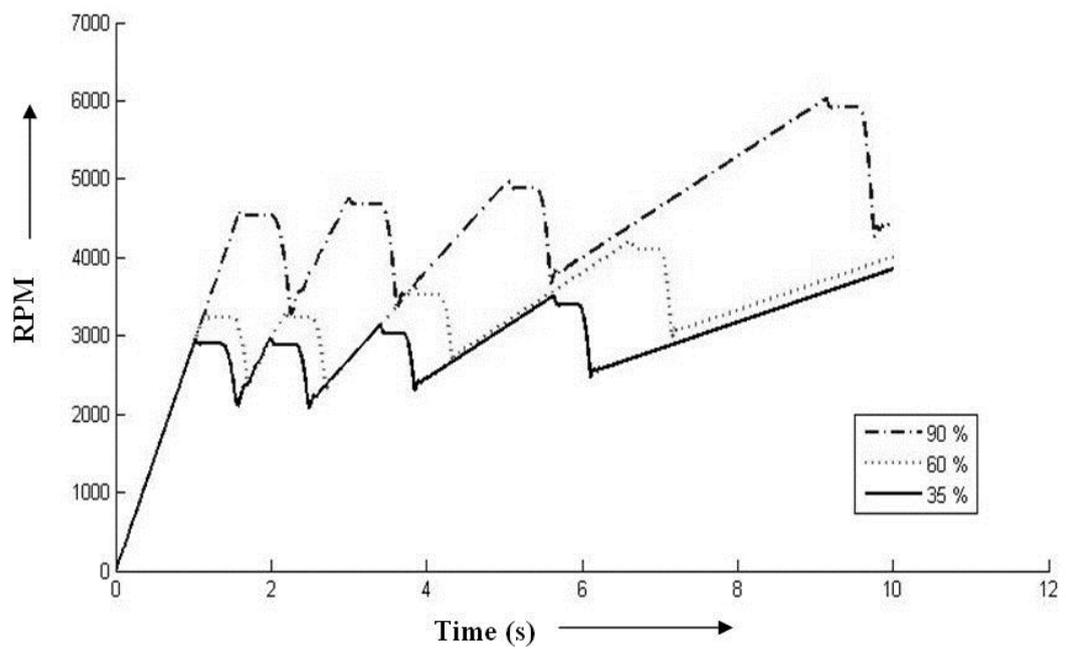
Figure 16. Time response of engine speed for different throttle positions.
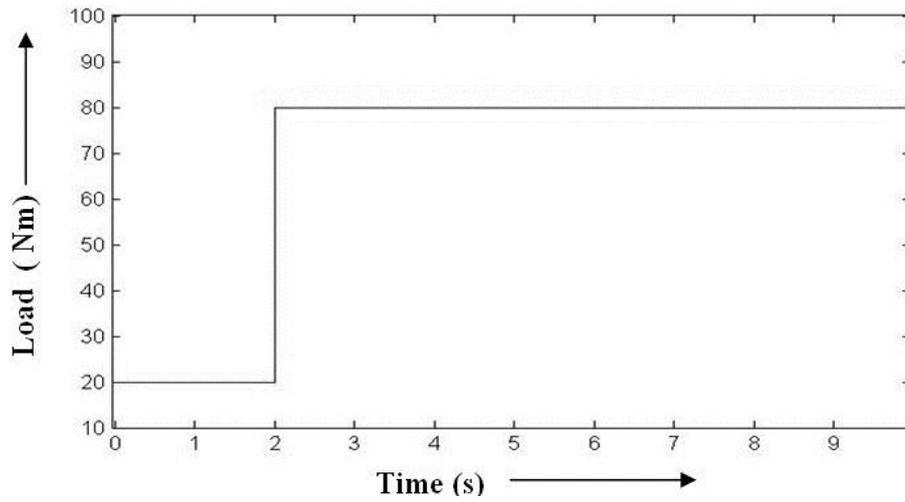
Figure 17: Sudden increase in load torque on vehicle.
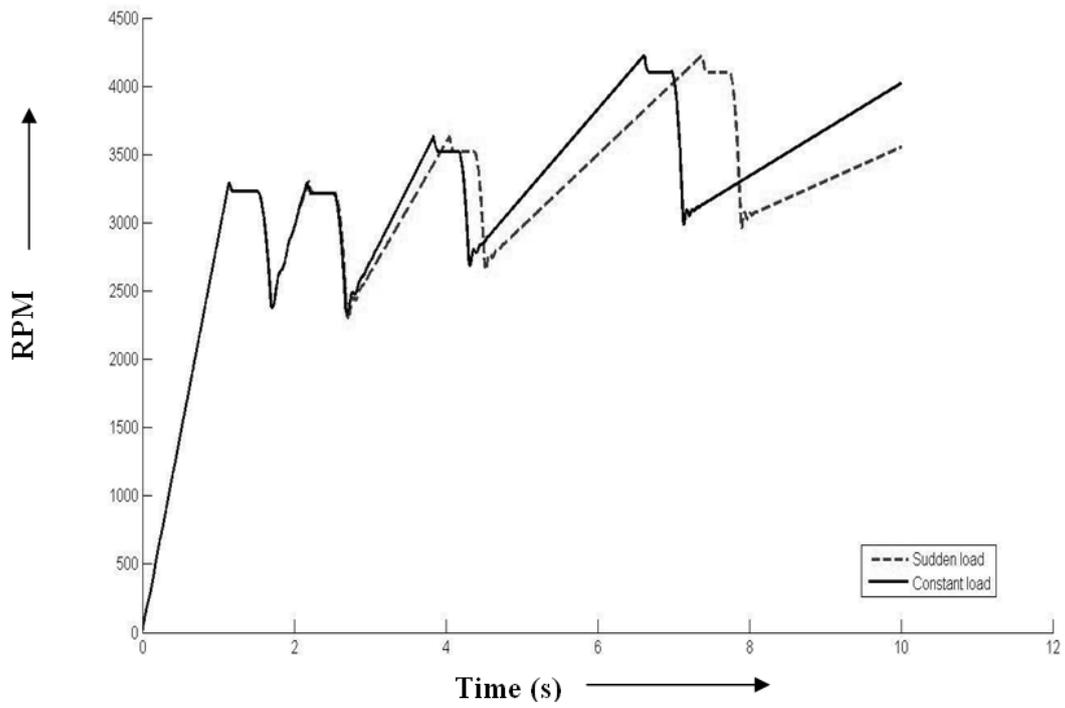
Figure 18: Gear-shift for sudden increment in load torque.
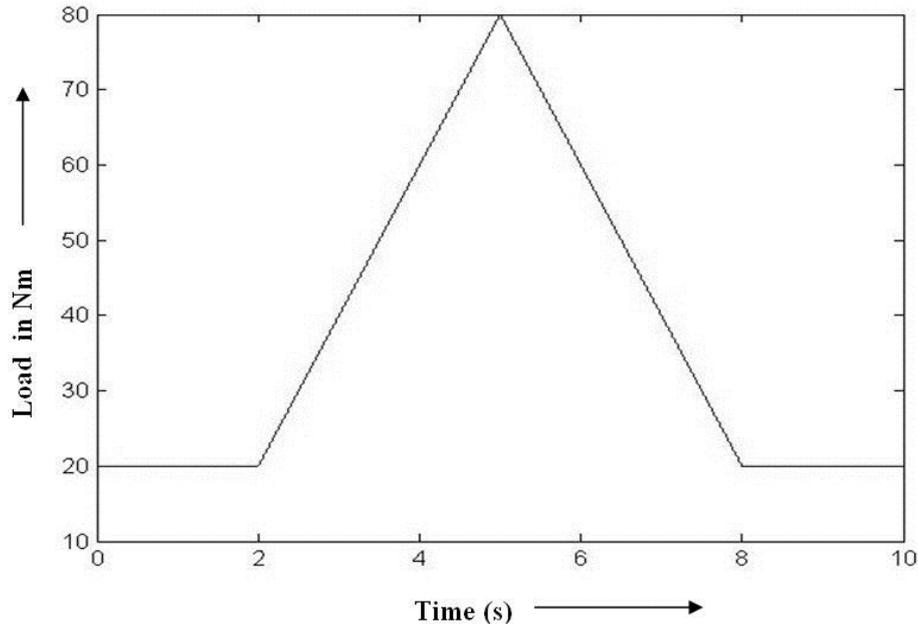
Figure 19. Varying load torque condition of vehicle.

For varying load torque, gear-shifting is shown in Figure 20 corresponding to varying load torque as shown in Figure 19. At 2nd second, load torque start increasing and increases up to 5th second to maximum load of 80 Nm after which it start decreasing to 20 Nm load torque up to 8th second. After that, it remains constant at 20 Nm. In Figure 20, dashed curve is for varying load torque and solid curve is representing constant load torque.
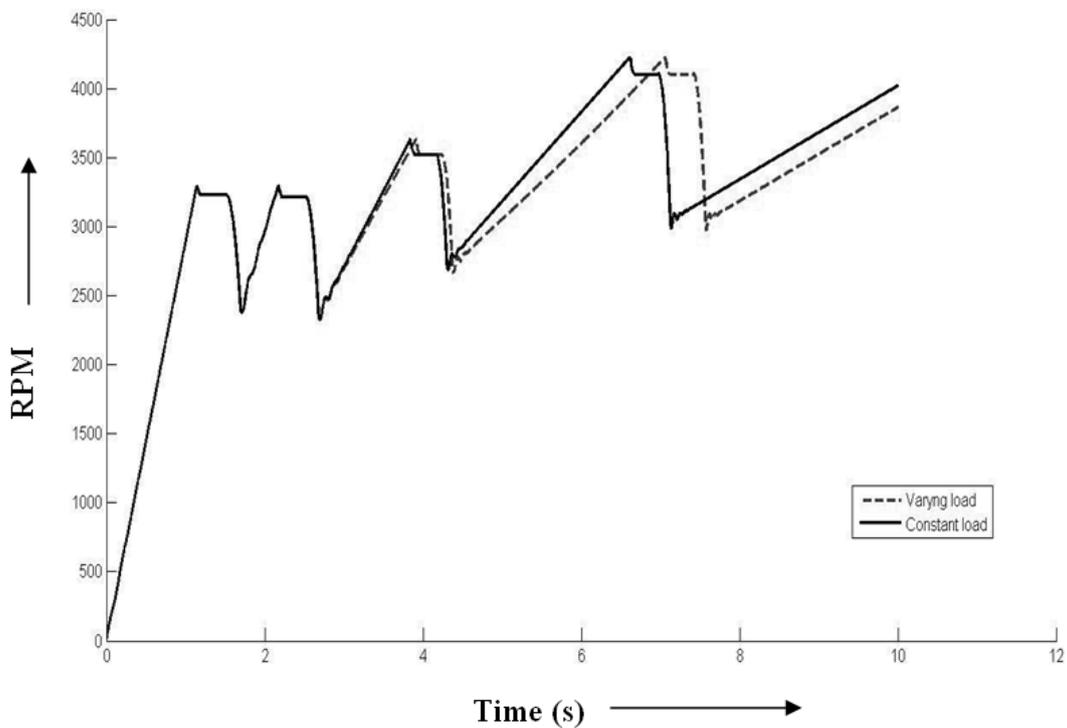
Figure 20: Gear-shift for varying load torque on vehicle.

CONCLUSION

A full driveline model is developed in MATLAB using state-space models of driveline. Gear shift strategy based on polynomial functions of gear shift curves is implemented in this driveline model. Simulation results of driveline model demonstrate that polynomial functions of gear shift curves are successful in shifting gears. The proposed model has been validated for different throttle positions, input torque values and load values. The effect of these parameters on gear-shift timing is obtained in simulation results presented. Further, the results show that the state space driveline model presented is able to define the driveline dynamics during the gear shifting and the proposed gear-shift strategy can shift gears successfully. Main conclusions drawn from this work are:

a) Optimal gear shift maps can be precisely modeled by a system of polynomial equations.
b) Polynomial equations based on gear shift maps can be used for gear shifting.
c) During clutch disengagement, engine speed decreases as only load torque due to clutch acts on crankshaft during this phase while clutch speed continues to increase due to vehicle inertia.
d) During synchronization, engine speed remains constant and clutch speed decreases due to applied torque at synchronizer.
e) During clutch engagement, engine speed decreases due to load torque acting at clutch while same torque but opposite in direction increases the clutch speed.

Gear-shifting strategy using polynomial functions can be conveniently validated practically on a vehicle. Using polynomials, gear-shifting can be made simpler as compared to the vehicles which use gear-shift maps directly for gear-shifting in AMT. This will lead to quick response using a simpler processor for TCU, improved performance of the vehicle and reduction in the cost of an AMT kit.

REFERENCES

[1]   Tseng CY, Yu CH. Advanced shifting control of synchronizer mechanisms for clutchless automatic manual transmission in an electric vehicle. Mechanism and Machine Theory. 2015;84:37–56.
[2]   Galvagno E, Velardocchia M, Vigliani A. Analysis and simulation of a torque assist automated manual transmission. Mechanical Systems and Signal Processing. 2011;25:1877–1886.
[3]   Pettersson M, Nielsen L. Gear shifting by engine control. IEEE Transactions on Control Systems Technology. 2000;8:495–507.
[4]   Zanasi R, Visconti A, Sandoni G, Morselli R. Dynamic modeling and control of a car transmission system. International Conference on Advanced Intelligent Mechatronics Proceedings, Como, Italy. pp:416–421; 2001.
[5]   Fredriksson J, Egardt B. Nonlinear control applied to gearshifting in automated manual transmissions. Proceedings of the 39th IEEE Conference on Decision and Control, Sydney, Australia, pp:444–449; 2000.
[6]   Zhong Z, Kong G, Yu Z, Chen X, Chen X, Xin X. Concept evaluation of a novel gear selector for automated manual transmissions. Mechanical Systems and Signal Processing. 2012;31:316–331.
[7]   Kim J, Park S, Seok C, Song H, Sung D, Lim C, Kim J, Kim H. Simulation of the shift force for a manual transmission. Proceedings of the Institution of Mechanical Engineers, pp:573–581; 2005.

[8]   Lucente G, Montanari M, Rossi C. Hybrid optimal control of an Automated Manual Transmission system. International Federation of Automatic Control. 2007;7:958–963.

[9]   Lin S, Chang S, Li B. Gearshift system design for automated manual transmission based on an electromagnetic actuator. International Conference on Electrical and Control Engineering, pp:2250–2253; 2011.

[10]   Yu Y, Wang G, Tian J. Analysis of electric acutator for light vehicle with AMT. International Symposium on Distributed Computing and Applications to Business, Engineering and Science, pp:667–6710; 2010.

[11]   Zhu X, Meng F, Zhang H, Cui Y. Robust driveshaft torque observer design for stepped ratio transmission in electric vehicles. Neurocomputing. 2015;164:262–271.

[12]   Galvagno E, Velardocchia M, Vigliani A. A model for a flywheel automatic assisted manual transmission. Mechanism and Machine Theory. 2009;44:1294–1305.

[13]   Kob MSC, Supriyo B, Tawi KB, Mazali II. Engagement slip controller development based on actuator displacement for an electro-mechanical friction clutch. International Journal of Automotive and Mechanical Engineering. 2015;11: 2664–2674.

[14]   Kim S, Choi S. Control-oriented modeling and torque estimations for vehicle driveline with dual-clutch transmission. Mechanism and Machine Theory. 2018;121:633–649.

[15]   Niu Q. Clutch control during starting of AMT. Procedia Engineering. 2010;7:447–452.

[16]   Qu J, Zhang Y. Control of clutch engagement for AMT based on fuzzy logic. 3rd International Symposium on Information Science and Engineering, pp. 47–50; 2010.

[17]   Wu G, Dong Z. Design, analysis and modeling of a novel hybrid powertrain system based on hybridized automated manual transmission. Mechanical Systems and Signal Processing. 2017;93:688–705.

[18]   Lv Y, Zhao Z, Gu J, Dong J. The research on the gear shift schedules for AMT in HEV. IEEE Intelligent Vehicles Symposium, pp. 722–729; 2009.

[19]   Hayashi K, Shimizu Y, Dote Y, Takayama A, Hirako A. Neuro fuzzy transmission control for automobile with variable loads. IEEE Transactions on Control Systems Technology. 1995;3:49–52.

[20]   Jianxue C. Automobile Transmission Shift Control based on MAX-MIN Ant Algorithm. TELKOMNIKA. 2013;11:4200–4207.

[21]   Yang Z. A method of optimal shift control based on pattern recognition and learning algorithm. 4th World Congress on Intelligent Control and Automation, pp. 955–959; 2002.

[22]   Niu Q, Fang Z, Wang K, Zhang G. The Theory and Application Study on Optimal Fuel Economy Shift Schedule. International Symposium on Computational Intelligence and Design. 2008;2:179–184.

[23]   Qu J, Zhang Y. Operation pattern recognition and control for an electric-hydraulic type AMT. International Symposium on Computational Intelligence and Design, pp. 302–305; 2009.

[24]   Qin G, Ge A, Lee JJ. Knowledge-Based Gear-Position Decision. IEEE Transactions on Intelligent Transportation Systems. 2004;5:121–126.

[25]   Lee HD, Sul SK, Cho HS, Lee JM. Advanced Gear-Shifting and Clutching Strategy for a Parallel-Hybrid Vehicle. IEEE Industry Applications Magazine. 2000;6:26–32.

[26]   Glielmo L, Iannelli L, Vacca V, Vasca F. Speed control for automated manual transmission with dry clutch. IEEE Conference on Decision and control.2004;2:1709–1714.